Quantifying the Role of Retardation Effects in Magnetic Plasmon Supporting Metal Nanoparticle Arrays

Nicholas P. Montoni, Steven C. Quillin, Charles Cherqui, and David J. Maisello*

Department of Chemistry, University of Washington, Seattle, WA 98195

E-mail: masiello@chem.washington.edu

Abstract

Magnetic plasmons, the collective response of cyclic arrangements of electric plasmon-supporting metal nanoparticles, have been of recent theoretical and experimental interest. As magnetic-plasmon-supporting aggregates are often large (hundreds of nanometers to microns in size), information takes time to propagate across such nanostructures. As a result, they are not well-described in the quasistatic limit with plasmon hybridization theory. In this Letter it is shown that for small magnetic oligomers the quasistatic approximation is sufficient, but, as the systems grow in size, retardation effects must be considered. The quasistatic tight-binding model can be manipulated to include retardation effects by utilizing the full electric field of a dipole. This fully retarded tight-binding model accurately predicts the energy-ordering of magnetic plasmon modes in agreement with full-wave simulations.

Keywords

plasmon, hybridization, magnetic, retardation

When two or more metal nanoparticles (MNPs) are brought together, their individual electric plasmons can hybridize to produce new, collective plasmon resonances.[1–4] Arranging three or more MNPs on the vertices of a polygon generates a collective mode that resembles a fictitious current loop and produces a sizeable magetic moment in the center of the polygon.[5–9] These aggregates can couple to and enhance the magnetic field of light, leading to applications such as solar cell enhancement,[10–12] biosensing and detection,[13–20] and information storage and propagation.[21–23]

Of recent interest has been the ability of magnetic plasmons, much like electric plasmons, to hybridize.[24] Similar to how a pair of electric plasmons can produce an electrically bright and an electrically dark mode, a pair of magnetic plasmons can produce a magnetically bright mode and a magnetically dark mode. This understanding opens up new routes to preferentially exciting magnetic and electric plasmons and distinguishing between the different plasmonic modes of a particular aggregate. Studies of the properties of magnetic plasmons have focused on plasmon propagation and hybridization, but have not sought to determine under what circumstances the magnetic plasmons of a system dominate its optical properties. Key to answering this question is the influence of retardation effects.

Much work has been done on magnetic plasmons in the quasistatic limit, which assumes that electromagnetic information propagates infinitely quickly. While retardation effects have been considered in studies of both large MNPs and infinite MNP arrays,[25–32] they have never been incorporated into models of intermediate-sized MNP arrays. Certainly, the single particle, single oligomer, and infinite system limits have been well-studied while the size regime in between is still relatively uncharted[**Kagan2017**]. This paper will show that, contrary to intuition, retardation effects play a significant role in the optical properties of magnetic-plasmon-supporting MNP aggregates int he intermediate size regime. It will be shown that by incorporating retardation effects into a simple model, the magnetic mode frequencies can be accurately predicted. Following this, it will be shown that the spectral order of the magnetic modes can be directly controlled, and that due to the specific radiative

properties of each magnetic mode, it is possible to track one of the magnetic modes as a function of energy, scale, and size. Finally, the magnetic and electric plasmons on single oligomers will be shown to interfere in such a way as to produce unidirectional radiation. The tracking of the magnetic modes and their interference with the electric modes is the key to determining when retardation effects must be included to produce an accurate model.

This work utilizes and augments a previously published tight-binding model.[9] The model in question maps the electric plasmon of each nanoparticle onto a harmonic oscillator and allows them to couple through quasistatic, near-field interactions using the Hamiltonian

$$\frac{H}{\hbar\omega_{\mathrm{sp}}} = \frac{1}{2}\sum_i \left[\mathbf{\Pi}_i^2 + \mathbf{Q}_i^2\right] - \frac{\alpha_{\mathrm{sp}}}{2}\sum_{i\neq j}\mathbf{Q}_i \cdot \mathbf{\Lambda}_{ij} \cdot \mathbf{Q}_j. \tag{1}$$

Here, ω_{sp} is the resonant frequency of the individual electric plasmons, the $\mathbf{\Pi}_i$ are the generalized momenta conjugate to the generalized coordinates $\mathbf{Q}_i$, α_{sp} is the polarizability of each individual MNP, and $\mathbf{\Lambda}_{ij}$ is the near-field dipole-dipole relay tensor. In this work, retardation effects are incorporated into the dipole-dipole relay tensor through the intermediate- and far-field terms in the dipole electric field as follows:

$$\mathbf{\Lambda}_{ij} = \left[\left(\frac{1}{r_{ij}^3} - \frac{\mathrm{i}\omega}{cr_{ij}^2}\right)\left(3\hat{\mathbf{n}}_{ij}\hat{\mathbf{n}}_{ij} - \mathbf{1}\right) + \frac{\omega^2}{c^2 r_{ij}}\left(\mathbf{1} - \hat{\mathbf{n}}_{ij}\hat{\mathbf{n}}_{ij}\right)\right] e^{\mathrm{i}\omega/cr}, \tag{2}$$

where r_{ij} is the distance between the i^{th} and j^{th} dipoles along the unit vector $\hat{\mathbf{n}}_{ij}$, $\mathbf{1}$ is the unit dyad, c is the speed of light, and ω is the collective frequency at which all of the dipoles oscillate. Using Equations 1 and 2, Hamilton's equations of motion,

$$\ddot{\mathbf{Q}}_i = -\mathbf{Q}_i + \sum_{j\neq i} \boldsymbol{Lambda}_{ij} \cdot \mathbf{Q}_j \tag{3}$$

can be found and the system of equations can be solved for the eigenvalues and eigenvectors of the nanoparticle array. The eigenvectors are the generalized coordinates corresponding to each dipole moment in the aggregate. It is important to note that because the eigenvalues, the collective frequencies, appear in the coupling terms, this will result in a system of

transcendental equations which must be solved iteratively.

In this paper, three model systems are considered. Following previous work, the model systems are constructed from fused, six-member rings of silver nanospheres, resembling conjugated hydrocarbon rings. The aggregates considered are a two-ring system, a linear three-ring system, and a triangular three-ring system. Solving for the magnetic eigenmodes of each system results in a set of eigenvectors for each mode which correspond to electric dipole moments. Figure **??** shows the oligomers, the dipole moments on each sphere, and the magnetic field distribution computed from[33]

$$\mathbf{B}_{\text{tot}}(\mathbf{r},\omega) = \frac{\omega^2}{c^2}\sum_j (\hat{\mathbf{n}}_j \times \mathbf{p}_j)\frac{e^{\mathrm{i}\omega/cr_j}}{r_j}\left(1 - \frac{c}{\mathrm{i}\omega r_j}\right). \tag{4}$$

From the magnetic field distributions and the orientation of electric dipoles, some key observations can be made about the magnetic modes. The in-phase magnetic mode of each oligomer (Figure **??**b, e, and h) has a net magnetic dipole, meaning it will couple to the magnetic field of light. The out-of-phase magnetic modes in Figure **??**a, d, f, and g all have net electric dipole moments, so they will interact with the electric field of light. The magnetic mode in Figure **??** has no dipole moments at all, making it optically dark. The classification of electrically bright and magnetically bright will play an important role in later discussion.

With the model producing the correct eigenmodes, it can now be used to show how properties such as scale of the oligomer and separation distance between MNPs impact the eigenvalues. To do this, a nearest neighbor distance is defined as $r_{nn} = (s+2)a_0$ where a_0 is the particle radius and s is a face-to-face distance in units of a_0. Figure **??**a shows the magnetic eigenmode frequencies as a function of oligomer scale. This is calculated by fixing the parameter $s = 1$ and varying a_0 from 1 nm to 30 nm. It can be seen for all three oligomers that at $a0 = 5$ nm the in-phase magnetic mode becomes the lowest in energy, contrary to predictions made by models in past work. Even more interesting is that the eigenmodes change spectral order again at 25 nm. Figure **??**a also includes comparison to simulation, showing that the model overestimates the eigenvalues by about 0.05 eV.

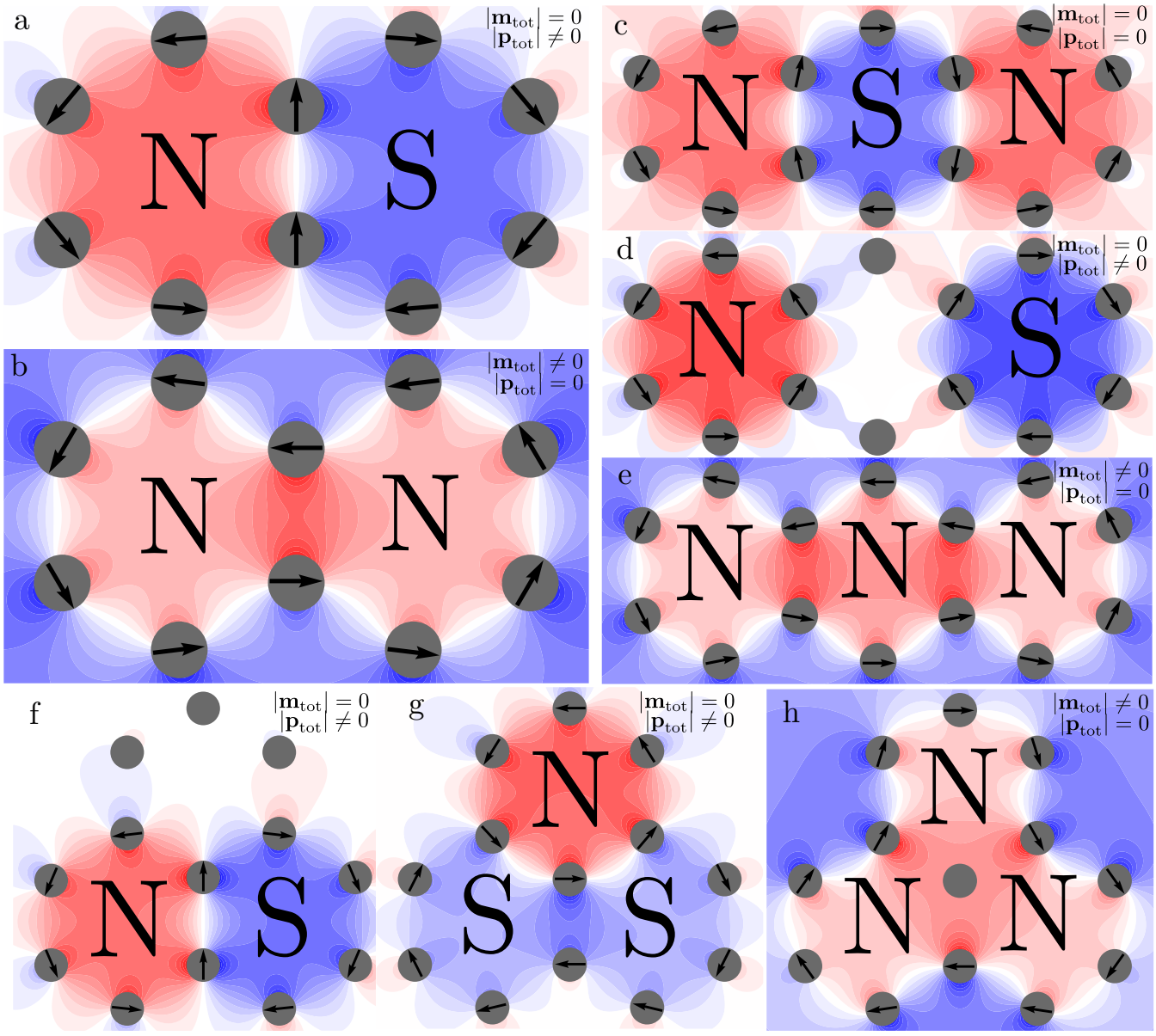
a
$|\mathbf{m}_{\rm tot}| = 0$
$|\mathbf{p}_{\rm tot}| \neq 0$
N
S
b
$|\mathbf{m}_{\rm tot}| \neq 0$
$|\mathbf{p}_{\rm tot}| = 0$
N
N
c
$|\mathbf{m}_{\rm tot}| = 0$
$|\mathbf{p}_{\rm tot}| = 0$
N
S
N
d
$|\mathbf{m}_{\rm tot}| = 0$
$|\mathbf{p}_{\rm tot}| \neq 0$
N
S
e
$|\mathbf{m}_{\rm tot}| \neq 0$
$|\mathbf{p}_{\rm tot}| = 0$
N
N
N
f
$|\mathbf{m}_{\rm tot}| = 0$
$|\mathbf{p}_{\rm tot}| \neq 0$
N
S
g
$|\mathbf{m}_{\rm tot}| = 0$
$|\mathbf{p}_{\rm tot}| \neq 0$
N
S
S
h
$|\mathbf{m}_{\rm tot}| \neq 0$
$|\mathbf{p}_{\rm tot}| = 0$
N
N
N

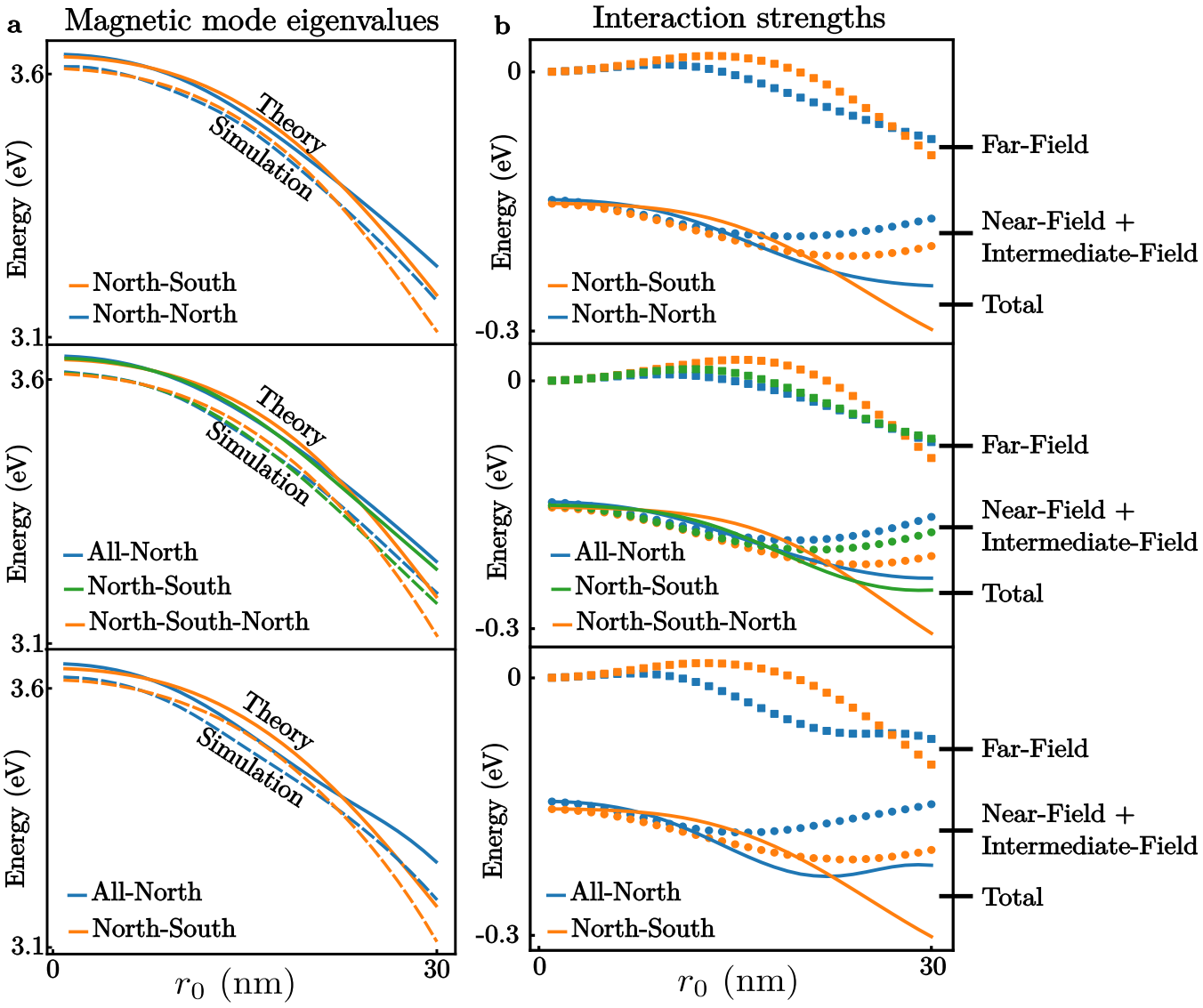
a
Magnetic mode eigenvalues
b
Interaction strengths
3.6
3.1
0
-0.3
30
Energy (eV)
r_0 (nm)
Theory
Simulation
North-South
North-North
All-North
North-South-North
Far-Field
Near-Field + Intermediate-Field
Total

Spectral switching of eigenmodes is counterintuitive and unexplored. In order to more fully explain why this could happen, Figure **??**b shows the total interaction strengths between dipoles in each eigenmode. More specifically, the total strength is computed, as well as the sum of the near- and intermediate-field strengths, followed by the far-field strength separately. This breakdown shows that the eigenmode crossings are due entirely to the far-field interaction. There are no crossings exhibited in the near- and intermediate-field terms, so these contribute only to net shifting of the eigenmodes. It is the change in relative magnitude of the far-field interaction that causes the eigenmodes to change spectral order. This is the most important point to take away from these plots: the far-field term is the magnetic term, and so it alone gives a measure of the importance of magnetic effects on these systems. And from these plots, it would seem that it becomes important for particles as small as 5 nm, and for separation distances between 15 nm and 50 nm.

Aggregate scale is not something that can be easily manipulated in real time in a laboratory, as it would require the refrabrication of a different aggregate for each experiment. However, recent research has focused on the ability of DNA and polymers to change shape and size in response to stimuli such as heat and pH[**cite Odom, Ginger, Schatz**]. Specifically, these techniques have been used to continuously and reversibly tune the aggregation scheme of a MNP array. Using this concept, the following set of calculations varies the nearest neighbor spacing, r_{nn} by varying s from 0 to 10 and keeping a_0 constant at 15 and 30 nm.

Figure **??**a shows the eigenvalues of each oligomer as a function of spacing for the 15 nm radius particles. As the space between particles increases, the magnetic modes collectively increase in energy, tending towards the single plasmon resonant frequency. The eigenvalues appear to cross and exhibit slight oscillatory motion. The crossings and oscillations are much more pronounced for the 30 nm particles (Figure **??**b). This is interesting because it shows that magnetic oligomers show a high degreee of spectral tunability. It can be seen that the energy order of the magnetic modes depends on a parameter that can be manipulated in

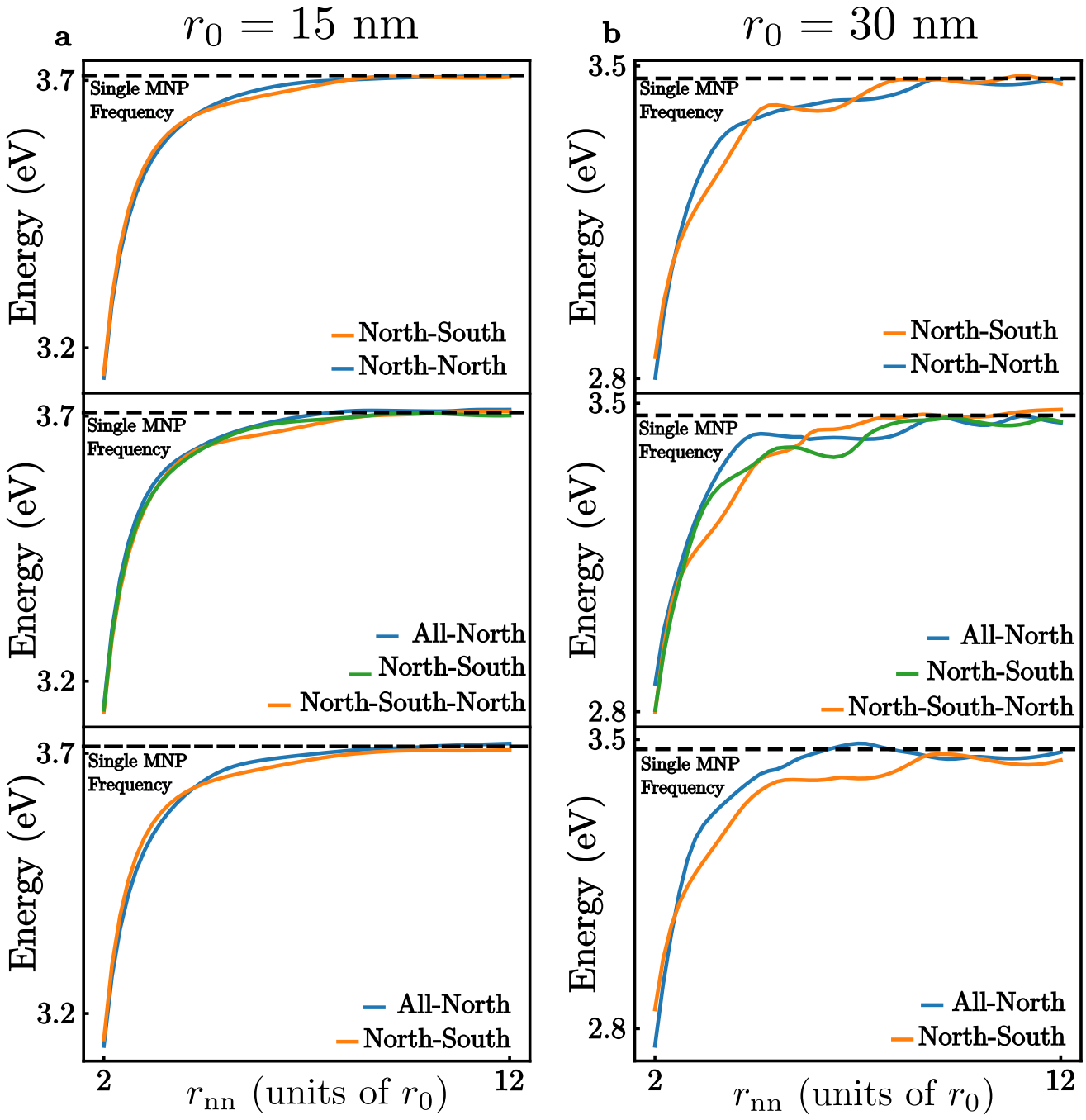
a
$r_0 = 15$ nm
b
$r_0 = 30$ nm
Energy (eV)
Single MNP Frequency
North-South
North-North
All-North
North-South-North
3.7
3.2
3.5
2.8
2
12
r_{nn} (units of r_0)

a laboratory. This versatility could be exploited to design optical magnetic switches and detectors.

There is a drawback in this line of reasoning, however. The splitting between the magnetic modes is very small, on the order of hundredths of electron volts, tenths at the most. In order to fully utilize magnetic oligomers, a technique is required to unravel these overlapping modes. Because the magnetic modes exhibit distinct, orthogonal magnetic and electric dipole moments, they can be individually or mutually excited by incoming light. Furthermore, because the dipole moments have orthogonal orientations, they scatter light in different directions. Finally, when the modes are mutually excited, they can interfere with each other to produce unidirectional radiation[**cite Kivshar**]. These properties are explored both as a way to observe the magnetic modes and as a way to quantify the importance of retardation effects. Because there are techniques that can measure the angular distribution of scattered light from a nanomaterial, this is presented as a way to infer the importance of the in-phase magnetic mode[**cite two papers measuring angular scattering**].

In planar plasmonic oligomers, the magnetic and electric collective plasmons are orthogonal to each other (see Figure **??**. Because of this, it is possible to probe multiple modes with a single laser polarization, specifically one in which the magnetic field of the incident light is directed through the rings of the oligomer. Because of the breadth and overlap of the magnetic modes, this will make it possible to observe both at once, but more importantly, this will make it possible to detect the point at which the magnetic plasmons dominate the spectrum.

Figure **??** shows this analysis in depth. The radiation pattern collected at the in-phase magnetic plasmon frequency of the twomer system is plotted in the plane containing the electric and magnetic field as a function of both scale and spacing. At small scalings, the scattered power appears to be entirely due to the electric plasmons. As the systems get larger, the magnetic scattered radiation dominates the pattern. This can be further seen in the scaling calculations, where the radiation pattern at a specific frequency changes from electric-

Scale

$r_{\mathrm{nn}} = 3.0 \times r_0$

$r_0 = 1$ nm

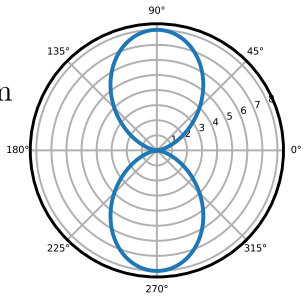

$r_0 = 5$ nm

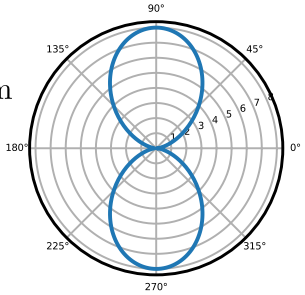

$r_0 = 10$ nm

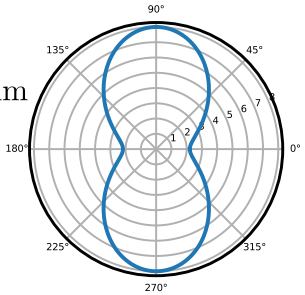

$r_0 = 15$ nm

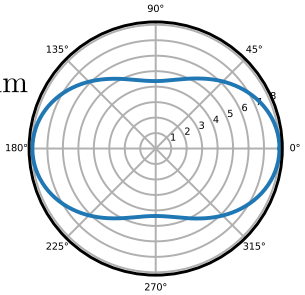

$r_0 = 20$ nm

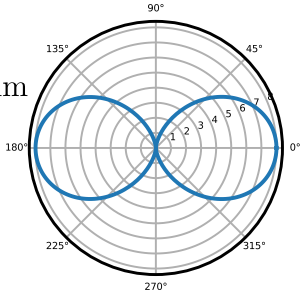

Spacing

$r_0 = 20$ nm

$r_{\mathrm{nn}} = 2.2 \times r_0$

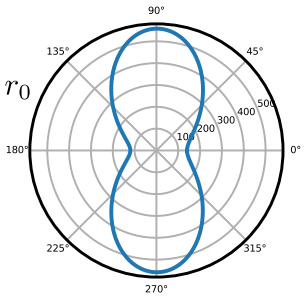

$r_{\mathrm{nn}} = 2.6 \times r_0$

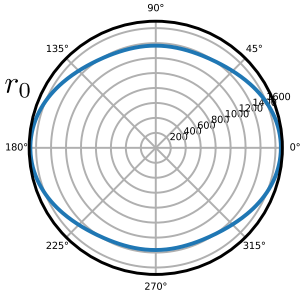

$r_{\mathrm{nn}} = 3.0 \times r_0$

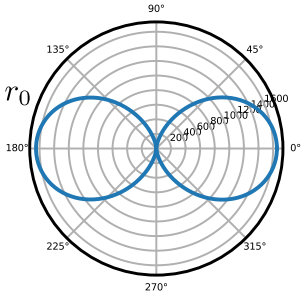

$r_{\mathrm{nn}} = 3.8 \times r_0$

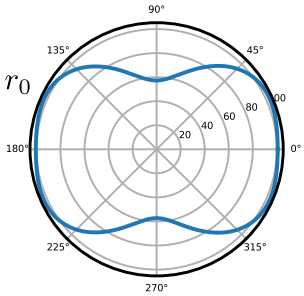

$r_{\mathrm{nn}} = 4.6 \times r_0$

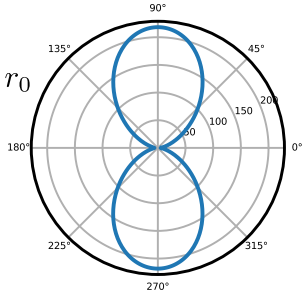

dominated to magnetic-dominated and back again. This is significant because it is the first step towards identifying and observing the phenomenon of magnetic mode switching. By watching a particular frequency and varying some system parameter, the radiation pattern can be shown to change. These results are even more significant because they show that even with particles as small as 10 nm in radius, retardation effects have a measureable impact on the optical properties of MNP aggregates.

Changing the plane in which radiation is collected from these systems leads to even more interesting results. Looking in the plane containing the magnetic field and the propogation direction of the incident light gives another measure of the role of retardation effects. When the magnetic and electric plasmons are of commensurate strength, their fields interfere destructively in some regions of space and constructively in others, leading to directionality in their emitted light. This can be seen in Figure **??**. As a function of scale, the radiation pattern can be seen to shift from pure electric dipole to unidirectional, and at large scalings, more magnetic in character. Similarly, as a function of spacing it can be seen that the unidirectionality dominates at certain energies and configurations. However, unlike the distinctive radiation patterns from the previous section, it would seem that once the magnetic plasmons are strong enough to interfere with the electric plasmons, the interference effects never truly go away, except in the case of particles infinitely far away from each other. According to equation [**PUT IN THAT EQUATION WHEN YOU'RE DONE AND SURE**], there is a sweet spot where the magnetic and electric plasmons can maximally interefere, and it occurs when they of nearly equal magnitude. This result is significant because it is the most convincing evidence yet that magnetic effects matter and contribute significantly to the optical properties of MNP aggregates. The point where the magnetic and electric plasmons maximally interfere is the point where magnetic, and by extension, retardation effects, matter most.

[**might consider field plots for longer and longer chains? just a few though, not overwhelming your readers with data. or maybe the ones in the field plots**

Scale

$r_{\mathrm{nn}} = 3.0 \times r_0$

Spacing

$r_0 = 20$ nm

$r_0 = 1$ nm

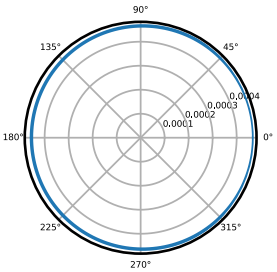

$r_{\mathrm{nn}} = 2.2 \times r_0$

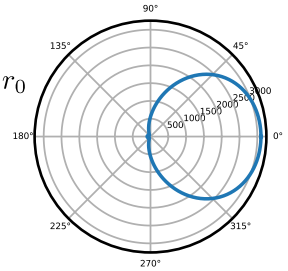

$r_0 = 5$ nm

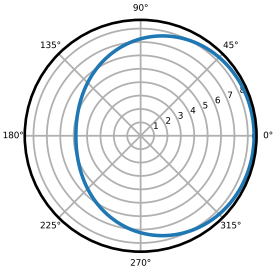

$r_{\mathrm{nn}} = 2.6 \times r_0$

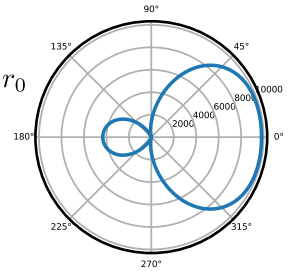

$r_0 = 10$ nm

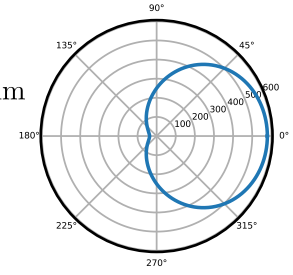

$r_{\mathrm{nn}} = 3.0 \times r_0$

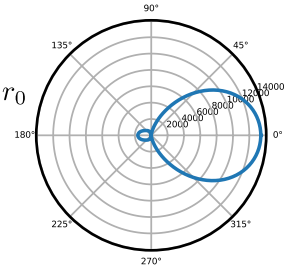

$r_0 = 15$ nm

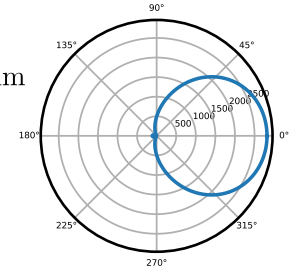

$r_{\mathrm{nn}} = 3.8 \times r_0$

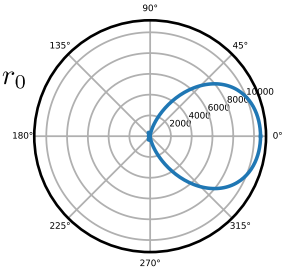

$r_0 = 20$ nm

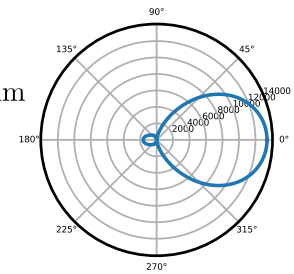

$r_{\mathrm{nn}} = 4.6 \times r_0$

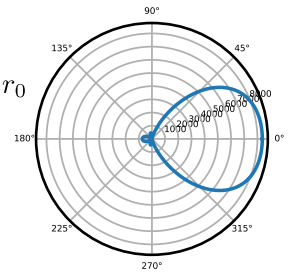

are enough. David is going to hate this.]

Even more interestingly, this phenomenon appears to break down with increasing length of the oligomer chain. Looking at chains of three, four, five, ten, and twenty oligomers, the beaming capabilities decrease as the chains become longer. This is further evidence of the idea the magnetic and electric dipole modes must be of commensurate strength in order to interfere and produce unidirectional radiation. Chains of magnetic oligomers behave much like particle-in-a-box states; this can be seen in the nodal structure of the twomer and linear threemer in Figure **??**. As the chains become longer, the magnetic modes will exhibit increasingly dilute field density, leading to weak interferences between modes. As a result, the radiation emitted by these structures loses its directionality. This is important because it emphasizes the significance of smaller magnetic oligomers as the perfect tools to understanding magnetic plasmons and retardation effects. The lack of unidirectionality of longer chains is displayed in Figure **??**.

Magnetic plasmon supporting aggregates consisting of few oligomers are excellent tools for analyzing the role of retardation effects on MNP aggregates. More conclusion.

Acknowledgement

CEI, Niket, Harrison, HPC/Hyak/Mox.

References

(1) Clippe, P.; Evrard, R.; Lucas, A. A. Aggregation Effect on the Infrared Absorption Spectrum of Small Ionic Crystals. *Phys. Rev. B* **1976**, *14*, 1715–1721.

(2) Aravind, P.; Nitzan, A.; Metiu, H. The Interaction between Electromagnetic Resonances and its Role in Spectroscopic Studies of Molecules Adsorbed on Colloidal Particles or Metal Spheres. *Surf. Sci.* **1981**, *110*, 189 – 204.

(3) Xu, Y. Electromagnetic Scattering by an Aggregate of Spheres. *Appl. Opt.* **1995**, *34*, 4573–4588.

(4) Mishchenko, M. I.; Mackowski, D. W.; Travis, L. D. Scattering of Light by Bispheres with Touching and Separated Components. *Appl. Opt.* **1995**, *34*, 4589–4599.

(5) Alù, A.; Salandrino, A.; Engheta, N. Negative Effective Permeability and Left-Handed Materials at Optical Frequencies. *Opt. Express* **2006**, *14*, 1557–1567.

(6) Alù, A.; Engheta, N. Dynamical Theory of Artificial Optical Magnetism Produced by Rings of Plasmonic Nanoparticles. *Phys. Rev. B* **2008**, *78*, 085112.

(7) Hentschel, M.; Dregely, D.; Vogelgesang, R.; Giessen, H.; Liu, N. Plasmonic Oligomers: The Role of Individual Particles in Collective Behavior. *ACS Nano* **2011**, *5*, 2042–2050, PMID: 21344858.

(8) Brandl, D. W.; Mirin, N. A.; Nordlander, P. Plasmon Modes of Nanosphere Trimers and Quadrumers. *J. Phys. Chem. B* **2006**, *110*, 12302–12310.

(9) Cherqui, C.; Bigelow, N. W.; Vaschillo, A.; Goldwyn, H.; Masiello, D. J. Combined Tight-Binding and Numerical Electrodynamics Understanding of the STEM/EELS Magneto-Optical Responses of Aromatic Plasmon-Supporting Metal Oligomers. *ACS Photonics* **2014**, *1*, 1013–1024.

(10) Graydon, O. Solar cells: Fano-enhanced performance. *Nat. Photonics* **2011**, *6*, 4.

(11) Le, K. Q.; Alu, A. Fano-Induced Solar Absorption Enhancement in Thin Organic Photovoltaic Cells. *Appl. Phys. Lett.* **2014**, *105*, 141118.

(12) Le, K. Q.; Bai, J. Enhanced Absorption Efficiency of Ultrathin Metamaterial Solar Absorbers by Plasmonic Fano Resonance. *JOSA B* **2015**, *32*, 595–600.

(13) Karaveli, S.; Zia, R. Strong Enhancement of Magnetic Dipole Emission in a Multilevel Electronic System. *Opt. Lett.* **2010**, *35*, 3318–3320.

(14) Noginova, N.; Zhu, G.; Mavy, M.; Noginov, M. Magnetic Dipole Based Systems for Probing Optical Magnetism. *J. Appl. Phys.* **2008**, *103*, 07E901.

(15) Wang, J.; Fan, C.; He, J.; Ding, P.; Liang, E.; Xue, Q. Double Fano Resonances Due to Interplay of Electric and Magnetic Plasmon Modes in Planar Plasmonic Structure with High Sensing Sensitivity. *Opt. Express* **2013**, *21*, 2236–2244.

(16) Zhu, Z.; Bai, B.; You, O.; Li, Q.; Fan, S. Fano Resonance Boosted Cascaded Optical Field Enhancement in a Plasmonic Nanoparticle-in-Cavity Nanoantenna Array and its SERS Application. *Light: Science and Applications* **2015**, *4*, e296.

(17) Lee, K.-L.; Huang, J.-B.; Chang, J.-W.; Wu, S.-H.; Wei, P.-K. Ultrasensitive Biosensors Using Enhanced Fano Resonances in Capped Gold Nanoslit Arrays. *Scientific Reports* **2015**, *5*, 8547.

(18) Wu, C.; Khanikaev, A. B.; Adato, R.; Arju, N.; Yanik, A. A.; Altug, H.; Shvets, G. Fano-Resonant Asymmetric Metamaterials for Ultrasensitive Spectroscopy and Identification of Molecular Monolayers. *Nat. Mat.* **2012**, *11*, 69–75.

(19) Cetin, A. E.; Altug, H. Fano Resonant Ring/Disk Plasmonic Nanocavities on Conducting Substrates for Advanced Biosensing. *ACS Nano* **2012**, *6*, 9989–9995.

(20) Zhang, S.; Bao, K.; Halas, N. J.; Xu, H.; Nordlander, P. Substrate-Induced Fano Resonances of a Plasmonic Nanocube: a Route to Increased-Sensitivity Localized Surface Plasmon Resonance Sensors Revealed. *Nano Lett.* **2011**, *11*, 1657–1663.

(21) Liu, H.; Genov, D. A.; Wu, D. M.; Liu, Y. M.; Steele, J. M.; Sun, C.; Zhu, S. N.; Zhang, X. Magnetic Plasmon Propagation Along a Chain of Connected Subwavelength Resonators at Infrared Frequencies. *Phys. Rev. Lett.* **2006**, *97*, 243902.

(22) Liu, N.; Mukherjee, S.; Bao, K.; Brown, L. V.; Dorfmüller, J.; Nordlander, P.;

Halas, N. J. Magnetic Plasmon Formation and Propagation in Artificial Aromatic Molecules. *Nano Lett.* **2011**, *12*, 364–369.

(23) Liu, N.; Mukherjee, S.; Bao, K.; Li, Y.; Brown, L. V.; Nordlander, P.; Halas, N. J. Manipulating Magnetic Plasmon Propagation in Metallic Nanocluster Networks. *ACS Nano* **2012**, *6*, 5482–5488.

(24) Cherqui, C.; Wu, Y.; Li, G.; Quillin, S. C.; Busche, J. A.; Thakkar, N.; West, C. A.; Montoni, N. P.; Rack, P. D.; Camden, J. P. .; Masiello, D. J. STEM/EELS Imaging of Magnetic Hybridization in Symmetric and Symmetry-Broken Plasmon Oligomer Dimers and All-Magnetic Fano Interference. *Nano Lett.* **2016**, *16*, 6668–6676, PMID: 27673696.

(25) Myroshnychenko, V.; Rodriguez-Fernandez, J.; Pastoriza-Santos, I.; Funston, A. M.; Novo, C.; Mulvaney, P.; Liz-Marzan, L. M.; Garcia de Abajo, F. J. Modelling the optical response of gold nanoparticles. *Chem. Soc. Rev.* **2008**, *37*, 1792–1805.

(26) Turner, M. D.; Hossain, M. M.; Gu, M. The Effects of Retardation on Plasmon Hybridization within Metallic Nanostructures. *New J. of Phys.* **2010**, *12*, 083062.

(27) Dahmen, C.; Schmidt, B.; von Plessen, G. Radiation Damping in Metal Nanoparticle Pairs. *Nano Lett.* **2007**, *7*, 318–322, PMID: 17243751.

(28) Rechberger, W.; Hohenau, A.; Leitner, A.; Krenn, J.; Lamprecht, B.; Aussenegg, F. Optical Properties of Two Interacting Gold Nanoparticles. *Opt. Commun.* **2003**, *220*, 137 – 141.

(29) Kottmann, J. P.; Martin, O. J. F. Retardation-Induced plasmon Resonances in Coupled Nanoparticles. *Opt. Lett.* **2001**, 1096–1098.

(30) Haynes, C. L.; McFarland, A. D.; Zhao, L.; Van Duyne, R. P.; Schatz, G. C.; Gunnarsson, L.; Prikulis, J.; Kasemo, B.; Käll, M. Nanoparticle Optics: The Importance of

Radiative Dipole Coupling in Two-Dimensional Nanoparticle Arrays. *J. Phys. Chem. B* **2003**, *107*, 7337–7342.

(31) Bouhelier, A.; Bachelot, R.; Im, J. S.; Wiederrecht, G. P.; Lerondel, G.; Kostcheev, S.; Royer, P. Electromagnetic Interactions in Plasmonic Nanoparticle Arrays. *J. Phys. Chem. B* **2005**, *109*, 3195–3198, PMID: 16851340.

(32) Kinnan, M. K.; Chumanov, G. Plasmon Coupling in Two-Dimensional Arrays of Silver Nanoparticles: II. Effect of the Particle Size and Interparticle Distance. *J. Phys. Chem. C* **2010**, *114*, 7496–7501.

(33) Jackson, J. D. *Classical Electrodynamics*, 3rd ed.; Wiley: New York, NY, 1999.

Graphical TOC Entry

Some journals require a graphical entry for the Table of Contents. This should be laid out "print ready" so that the sizing of the text is correct.
Inside the `tocentry` environment, the font used is Helvetica 8 pt, as required by *Journal of the American Chemical Society*.
The surrounding frame is 9 cm by 3.5 cm, which is the maximum permitted for *Journal of the American Chemical Society* graphical table of content entries. The box will not resize if the content is too big: instead it will overflow the edge of the box.
This box and the associated title will always be printed on a separate page at the end of the document.